Theoretical and Applied Climatology
https://doi.org/10.1007/s00704-018-2681-4

ORIGINAL PAPER

Using self-organizing maps to identify the South Asian seasonal cycle

Md Rafiqul Islam[1] · Scott C. Sheridan[1] · Cameron C. Lee[1]

Received: 31 October 2017 / Accepted: 15 October 2018

Abstract

A synoptic climatological approach using the self-organizing maps (SOMs) technique has been used to identify South Asian seasonality, by categorizing atmospheric patterns for each of five near-surface variables. This research mainly focused on showing the general climatology of the monsoonal seasonal cycle through four traditional seasons (winter, pre-monsoon, monsoon, and post-monsoon) and the transitions between each of these seasons, highlighting spatiotemporal variability. For each variable, a 9 × 9 SOM was created using surface-level reanalysis data. Each node in each SOM is assigned to a season or a seasonal transition, based on defined standard criteria. The SOM-based synoptic approach helps to increase our understanding and visualization of the different atmospheric conditions and their seasonal cycle of the South Asian climate, such as a complete reversal of mean sea-level pressure over the course of the year, with high pressure over the land in winter and low pressure in the summer, and a clear seasonal cycle in wind direction with cyclonic and anticyclonic circulations in different seasons creating a greater wind speed over the ocean than the land.

1 Introduction

The South Asian climate system is enormously affected by the monsoon climate environment, most famously called the Indian monsoon. It is one of the most important tropical climate systems on Earth. A monsoon is a seasonal change in the fundamental wind direction that usually brings a change in weather. Although it is traditionally defined as a seasonally reversing wind that comes with corresponding changes in precipitation (Ramage 1971), it is also used to describe seasonal changes in atmospheric circulation and precipitation associated with the asymmetric heating of land and sea (Pant and Kumar 1997). However, the South Asian monsoon is not a simple response to heating but a more complex interaction of topography, influenced by the shape of the continent, winds, and the sea. Two seasons (the summer monsoon and winter monsoon) dominate the climate in this region, accompanied by other two transitional seasons (pre-monsoon or spring and post-monsoon or autumn) in between, which follow the general seasonality of the Northern Hemisphere. Most of the climate research in this region have mainly focused on the definition of only the summer monsoon season (Pant and Kumar 1997), especially using rainfall distributions and patterns (Krishnamurthy and Shukla 2000; Kumar et al. 1995), the relationship of wind to rainfall (Mukherjee et al. 1985; Bhalme et al. 1987), and sea surface temperature (Rao and Goswami 1988) to rainfall (Rasmusson and Carpenter 1982). Another possible means of studying the seasonal cycle is the use of synoptic climatological analysis to identify atmospheric patterns and their seasonality. While the synoptic approach has not been applied to the South Asian monsoon climate system as a whole, Chattopadhyay et al. (2008) used SOMs for predicting different phases and real-time extended-range prediction of monsoon inter-seasonal oscillation. While much research in this region has been conducted to examine the monsoon season and rainfall variability, no research has been found which has focused on overall seasonal delineation of this region. Therefore, the goal of this research is to apply the self-organizing maps technique using several distinct atmospheric variables to identify both the four conventional seasons and the transitions between seasons through atmospheric patterns, in order to gain an understanding of the general climatology of the South Asian region and its spatiotemporal variability.

✉ Md Rafiqul Islam
mislam2@kent.edu

[1] Department of Geography, Kent State University, 800 E Summit St, Kent, OH 44240, USA

Published online: 25 October 2018

2 Background

2.1 Synoptic climatology and self-organizing maps (SOMs)

Synoptic climatology includes the study of the atmospheric circulation and its relationship with the local and the regional climate. It also deals with the movement of air masses, pressure centers, weather systems, and fronts across time and space (Sheridan and Lee 2014). Fundamentally, synoptic climatological approaches take one of two perspectives: circulation-to-environment, which aims to identify the complete range of atmospheric patterns over the study area and then applies these patterns to an environmental response, and environment-to-circulation, which investigates only the range of atmospheric patterns associated with a specific environmental condition (Yarnal 1993). Over time, a number of classification methods have been developed and implemented Barry and Perry 1973a, b, 2001; Sheridan 2002; Demuzere et al. 2009; Lee and Sheridan 2015) providing a general framework to understand the succession of daily meteorological situations. The synoptic climatological approach is mostly reserved for the mid-latitudes where the atmospheric circulation is mainly defined by synoptic-scale events. This approach has not often been applied to tropical monsoon areas because the climate in these regions is mostly defined by the occurrences of mesoscale convective systems (Gueye et al. 2011) which are often independent of synoptic-scale patterns. However, synoptic weather types have been shown to provide information on local-scale rainfall occurrence (Deme et al. 2003) of monsoon circulation systems.

During the last two decades, one of the most widely used methods in synoptic climatological research has been cluster analysis, which is preceded by a principal component analysis (PCA). Normally PCA serves as a data reduction technique while also producing orthogonal principal component scores—a necessary characteristic of variables entering a cluster analysis (Yarnal 1993); the subsequent cluster analysis groups the principal component scores (or a subset of them) into a classification (Barry and Perry 2001; Yarnal 1993). Although this method is utilized in different applications and easily replicable in statistical packages, it generally does not organize the atmospheric patterns into a continuum of the discrete realizations of an atmospheric system (Sheridan and Lee 2011). Kohonen (1998) presented significant details of self-organizing maps (SOMs) which eventually lead to the development of an organizational method for atmospheric pattern classification, Hewitson and Crane (2002) then introduced the concept of SOMs in terms of their utility to synoptic climatology.

Using an S-mode decomposition of the data, the SOM methodology utilizes a neural network algorithm whereby a two-dimensional array (or lattice) is initialized to span the two leading principal components (PCs) of the input data, and through multiple iterations, node positions are adjusted and the lattice morphs around the cloud of input data points on the PC axes. Unlike other clustering methods (e.g., PCA and cluster analysis), SOMs do not need a priori decisions on the multivariate data distribution because they are trained to learn the data distribution and structure, and most importantly, the resulting maps are organized such that similar synoptic patterns or types are adjacent on the lattice. Further, the SOM algorithm naturally places more nodes in areas of high data density and fewer nodes in areas of low data density (Cassano et al. 2005). The user determines the size of the SOM depending upon the objectives of the study, such as the degree of generalization (Hewitson and Crane 2002). Training of the SOM is accomplished by two phases of learning. In the first phase, a large initial radius is used to develop the broad mapping across the array of nodes (Hewitson and Crane 2002), and the second phase develops the finer details of mapping where the radius is progressively reduced. Each SOM node is representative of the nearby cloud of the multi-dimensional data set, and thus, the nodes of the SOM identify the primary features of the synoptic-scale circulation of a region and represent a nonlinear continuum of patterns whereby similar patterns are adjacent to one another on the lattice, and very different patterns are further apart (Hewitson and Crane 2002; Cassano et al. 2015).

2.2 Application of self-organizing map techniques

The improved visualization of SOMs makes them a popular tool in research with climatological applications (Sheridan and Lee 2011), particularly when looking at extreme events or circulation-precipitation relationships (e.g., Cavazos 2000; Michaelides et al. 2001; Lynch et al. 2006; Hewitson and Crane 2002; Cassano and Cassano 2010). Cassano and Cassano (2010) used this method to create a synoptic climatology for northwestern North America and adjacent regions, creating a SOM of sea-level pressure patterns to identify the relationship between precipitation characteristics and synoptic patterns, and subsequently (Cassano et al. 2015, 2017) the extreme winter temperatures in the Arctic using surface circulation. Recently, in a case study in Australia, Gibson et al. (2017) shows how a diverse range of patterns represents the synoptic conditions during heat waves. Swales et al. (2016) used SOMs to examine mechanisms for extreme rainfall in the USA on vertically integrated water vapor transport. Horton et al. (2015) provided evidence for changes in the frequency of geopotential height patterns affecting extreme temperature trends across the Northern Hemisphere mid-latitudinal regions. Hewitson and Crane (2002) classify synoptic patterns over the east coast of the USA and relate these patterns to daily precipitation at State College, Pennsylvania. Cavazos (2000) identifies and classifies the extreme anomalies associated with local precipitation events in Central America and the Balkans. SOMs have also been used in the higher latitudes as a basis for understanding the synoptic forcing of Greenland precipitation trends (Schuenemann and Cassano 2009) to find out various locations of cyclones and anticyclones in the North Atlantic domain. SOMs have also been used in research (Cassano et al. 2006; Finnis et al. 2009; Lynch et al. 2006; Tozuka et al. 2008) to validate General Circulation Model (GCM) output (Sheridan and Lee 2010). Some of the GCM validation studies (Cassano et al. 2006; Lynch et al. 2006) compared the performance of SOMs and GCMs with synoptic SLP frequencies. They also applied SOMs to GCM output to examine how models generate precipitation scenarios. Crane and Hewitson (2003) used SOMs in analyzing precipitation and several other studies have examined aspects of monsoon precipitation using SOMs. A SOM of sea-level pressure has been used to assess the Australian monsoon and its precipitation-synoptic type relationship (Verdon-Kidd and Kiem 2009), and trends in Australian precipitation (Alexander et al. 2010; Hope et al. 2006). Gueye et al. (2011) looked at the key synoptic weather patterns in the Senegal monsoon using a nine-SOM array, and Cavazos et al. (2002) assessed variability, strength, and mode of Arizona monsoon circulation. Chattopadhyay et al. (2008) studied Indian intra-seasonal monsoon oscillation (ISO) by creating two different dimensions of SOMs, looking at similarities and differences within the spatial and temporal evolution of active and break phases of summer monsoon rainfall.

3 Data and methods

3.1 Data

Daily mean data for five near-surface atmospheric variables (sea-level pressure, wind (sig995), temperature (sig995), relative humidity (sig995), and precipitation) have been obtained from the NCEP-NCAR Reanalysis 1 project (Kalnay et al. 1996). The spatial resolution of these data is 2.5° × 2.5° (latitude × longitude) and selected grid points extend from 0° to 40° N and 60° to 100° E (Fig. 1) for 69 years (1948–2016). The NCEP-NCAR Reanalysis is useful for analyzing large scale and inter-annual variability (Janowiak et al. 1998), and this data had been acquired with advanced quality control and monitoring system (Kalnay et al. 1996). There is some previous research that used NCEP-NCAR data (e.g. Kripalani et al. 2003) for Indian monsoon rainfall and snow cover of Himalaya mountain ranges. Surface-level atmospheric variables have been used because the data are historically more reliable and most of the atmospheric interactions with the environment take place at this level. Multiple atmospheric variables were acquired in order to examine the seasonality of each of these independently and to evaluate whether this method can successfully replicate seasonality across different key atmospheric variables. Further, these variables are often used colloquially to characterize the daily weather and also have discernable effects on the monsoon climate system. To validate the synoptic classification to local and regional climate outcomes, precipitation data for Kerala and Bangladesh are also obtained from the same source with 1.25° × 1.25° resolution.

3.2 SOM methodology

The selection of the dimension and number of nodes in SOMs depends upon (1) how the user wants to visualize the data set regarding the objective of their research, (2) the distribution and the properties of the variable, and (3) the density distribution of the data set within the range to visualize the expected classification. As the primary goal of making the SOM in this research is for seasonal delineation, it is crucial to decide the dimensions of the SOM and an optimal number of nodes where the traditional seasonality and traditional periods between these seasons can both be discerned clearly within the SOM patterns. As such, different dimensions (e.g., 4 × 3, 6 × 4, 8 × 7, 9 × 9, 10 × 10, and 20 × 20) of SOMs were tested in terms of their ability to visualize the seasonality. The lattices with a smaller number of nodes show distinct patterns, but distinguishing different seasons is difficult, as it provides vague information, since there is greater within-node variability, making it difficult to delineate seasons. For instance, if we want to classify the data set into four seasons with a 4 × 3 SOM, we may have several nodes which identify one or two seasons distinctly, but for most of the cases not only is the transition between seasons quite difficult to identify but also a significant number of nodes of the SOM may belong to multiple seasons rather than a single season which fails to achieve the objective of the research. On the other hand, a SOM lattice with a very large number of nodes results in an inability to distinguish seasonal changes (e.g., where one season starts and another ends) because many nodes represent similar patterns that fail to account for seasonal distinction. Thus, after trial and error, ultimately a 9 × 9 SOM was chosen to visualize four distinct seasons (winter, pre-monsoon, monsoon, and post-monsoon). The choice of 9 × 9 SOMs with 81 cluster nodes was based on the fact that there are an optimal number of nodes to visualize the seasonal transition clearly, while also maintaining the adequate information within each of the seasons. Further, 81 cluster nodes were uniformly set out for all of the variables so that seasonal delineations can be compared among the variables. Among various other possible initiation topologies, the "gridtop" topology function was selected for consistency with most other SOM-based climate research (e.g., Hewitson and Crane 2002; Cassano et al. 2015). Matlab 2016a was used to perform a two-dimensional PCA and create SOMs of all variables, and the following settings were applied:

Ordering phase learning rate = 0.90
Tuning phase learning rate = 0.02
Distance learning function = link dist.
Iterations = number of days of the data set

3.3 Seasonal delineation

While traditionally there are six seasons in the monsoon climate system, defining only six seasons via circulation pattern classification was not convincing, as frequently a single node spanned multiple seasons, making seasonal partitioning difficult to visualize. Therefore, similar to the seasons of many mid-latitude northern hemisphere locations, meteorologically, a year in the monsoon climate system was determined to consist of four distinct seasons: winter, pre-monsoon, monsoon, and post-monsoon. The SOMs partitioned these four seasons with each season generally occupying one contiguous part of the overall matrix. Each of the season's lengths are considered based on an initial definition (Table 1) of the conventional months of the year, divided into full-length seasonal months (months clearly dominated by one season) and the transitional months (in which one season typically transitions to another).

After applying the primary seasonal criteria above, each of the SOMs nodes is then considered for assignment into a season based on the percentage of total days for each node that occur within a given month. Each node was then grouped into a season based upon the following ordered criteria.

- Firstly, if at least 70% of the days classified into a particular node fall into the full-length months of one season, it is considered a node for that season. The specific threshold of 70% was chosen as it yields the best classification of seasons overall. Greater or lower thresholds leave a significant number of nodes undefined.
- Secondly, if a node does not meet the first criterion (e.g., more than 30% of the day misclassified with falling out of the full-length seasonal months), it is initially called a disputed or transitional node between the seasons. To classify these nodes into a season, the frequency of the node within full-length seasonal months as well as the adjacent transitional months is summed. If this sum is more than 70% of all days classified as a particular node, the respective node falls into this season. If more than one season ends up with over 70% of the node's frequency using this method, then the node is assigned to the season with greater overall value.
- Thirdly (in a very few cases), a node has most of its days classified into transitional months. In this case, then two additional standards are taken into consideration to decide the season associated with that particular transitional node:

  1. The two seasons adjacent to the transitional month with the highest frequency of days are examined, and the node is classified into the season with the greater percentage of circulation days.
  2. Specifically for the monsoon season, the domain-wide mean precipitation for node has been calculated, and if the mean precipitation of the transitional node is greater than at least one other monsoon node, then it is classified as monsoon; otherwise, it is pre-monsoon or post-monsoon based on the peak seasonality.

Through applying the above criteria, the SOM classifications of atmospheric patterns can be used for seasonal classification.

4 Results

4.1 Sea-level pressure

Variations in sea-level pressure are one of the most important determinants of seasonal change in the South Asian monsoon climate. The SOM organizes the monsoon and winter season distinctly in the right and left sides of the map in Fig. 2, (the frequency by month, mean sea-level pressure and mean precipitation field over sea-level pressure SOM are shown in Fig. 3, and mean field of each season and transition in Fig. 4), respectively, while pre-monsoon and post-monsoon both occupy the central part of the SOM with a mixed array, because of the nature of the data: the sea-level pressure patterns in the two seasons are similar. The organization of the distributions of circulation patterns in the SOM array shows high pressure patterns (winter, right side of the map) gradually transitioning to low pressure patterns (monsoon, left side of the map) in a sequence so that seasons themselves can easily be distinguished. Within the context of the seasonal cycle, the SOM can aid in visualizing season-to-season variability. The winter nodes all depict the broad north-to-south pressure gradient, with SLP between 1030 and 1040 mb over the Tibetan Plateau decreasing to 1015 mb southwards. As the season progress, several winter nodes (e.g., 2, 29, 37, and 75) show decreases in pressure, particularly over parts of the Tibetan Plateau and the Indian peninsula. The decreasing pressure starts to become more prevalent as the pre-monsoon season progresses, and in some nodes that dominate in March and April (e.g., nodes 4, 23, 77, and 78), this low-pressure belt extends from over southern Bangladesh westward to the Thar

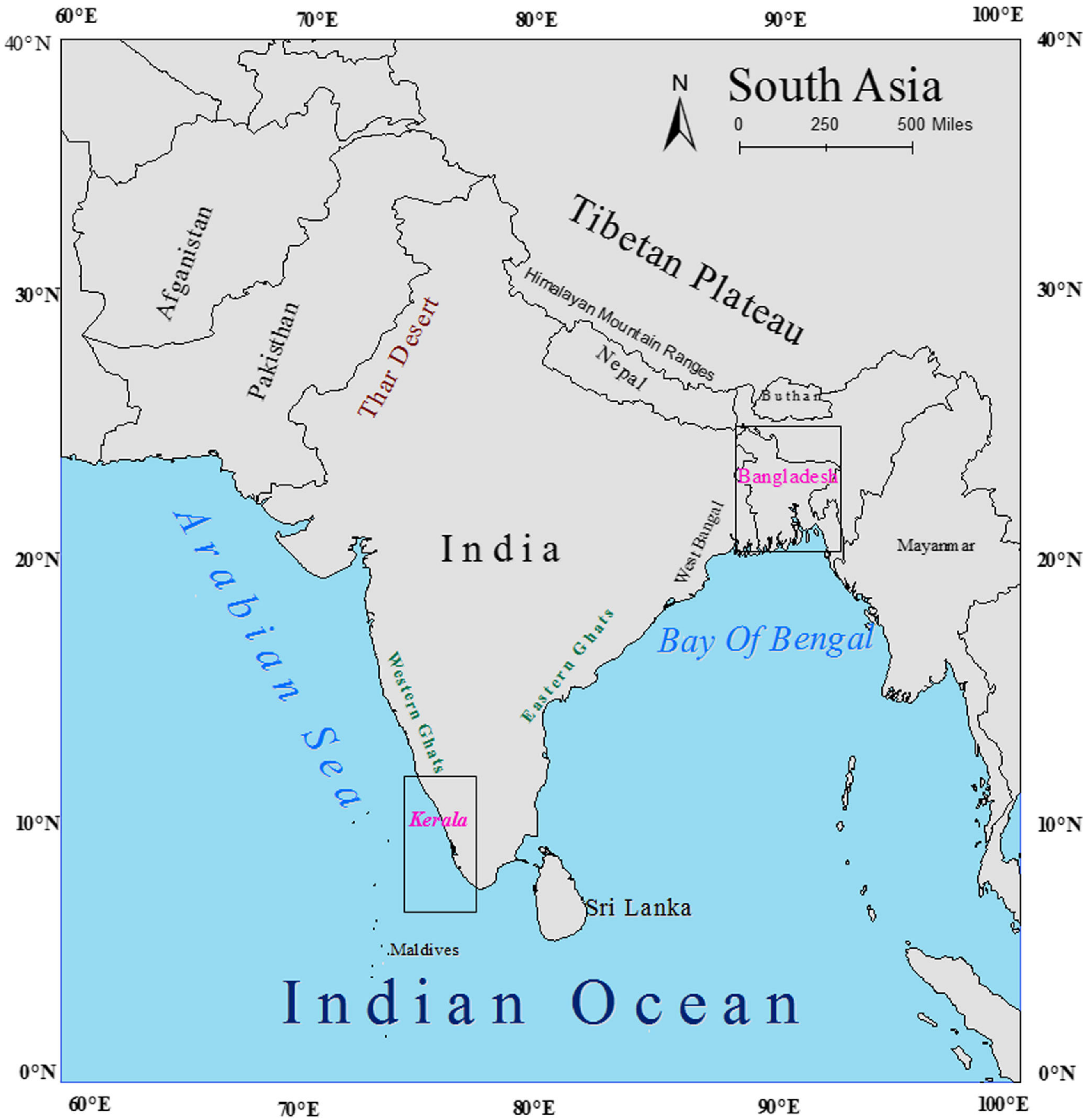

Fig. 1 South Asia and two local region of interest, Kerala and Bangladesh

Desert. At the next stage of the seasonal cycle, the monsoon season depicts low pressure over India (e.g., nodes 42, 43, 51, and 71), and by June and July nodes (e.g., 62, 63, 72, and 81) show an extension of the low-pressure belt towards the southwest (Arabian Sea and Pakistan). Towards the end of the monsoon, several nodes (e.g., 7 and 17) that dominate in August

Table 1 Initial definition of seasonal month of a year

Initial definition of seasonal month of a year											
Pre-monsoon			Monsoon				Post-monsoon		Winter		
Full-length month		Transition	Full-length month			Transition	Full-length month	Transition	Full-length month		Transition
March	April	May	June	July	August	September	October	November	December	January	February

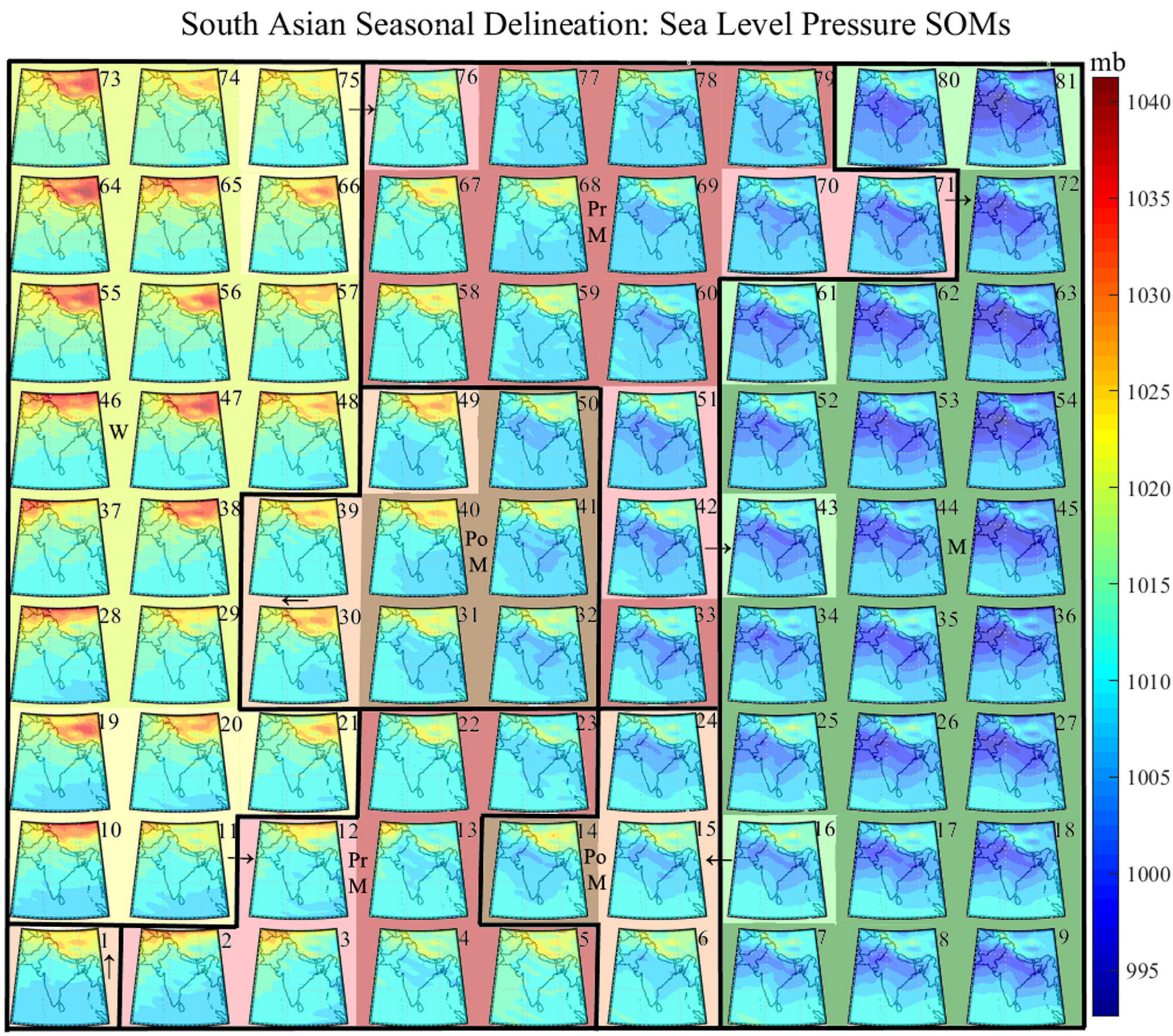

Fig. 2 SOM lattice for sea-level pressure. Enclosed shade areas denote the different seasons (Pr-M = pre-monsoon (red), M = monsoon (green), Po-M = Post-monsoon (brown), and W = Winter (yellow), while paler shades of each color denote the transitional nodes and direction of the arrow denotes that the node tend to shift to the following season or fall into the season from prior season. Seasonal nodes are arranged as a way that monsoon with low pressure is in the left, winter with high pressure is in the right, and pre-monsoon and post-monsoon are in a mixed array placed in the middle of the SOM

clearly show the filling of the low pressure belt, and some nodes (e.g., 16) in September show further filling with the high-pressure belt over the Himalayas as well as the Tibetan Plateau. This transition persists into the post-monsoon, as the high pressure gradually starts to take stronger hold over the land (e.g., nodes 6, 14, 15, and 16).

4.2 Wind

The SOM for wind in Fig. 5 (with additional analysis in Figs. 6 and 7) also depicts four distinct seasons and their transitions clearly: the winter nodes are organized on the lower left side, the pre-monsoon on the lower right side, the monsoon on the upper right side, and the post-monsoon in the upper left side of the map. While in the sea-level pressure SOM, the pre-monsoon and the post-monsoon seasonal nodes are together in a mixed array, the wind SOM not only organizes each of the seasons separately but also in such a way that the seasonal cycle can be visualized in a cyclic order across the SOM array. Indicative of this cycle, the winter nodes that dominate the beginning of the calendar year (e.g., nodes 10, 11, 12, 13, 19, 20, 21, and 22) depict a northeasterly wind over both branches of the monsoon system. The nodes associated with the transition to pre-monsoon in February (e.g., nodes 5, 6, 14, and 15) show these winds beginning to decrease, and in the pre-monsoon in March (e.g., nodes 8, 9, 16, and 24), the winter

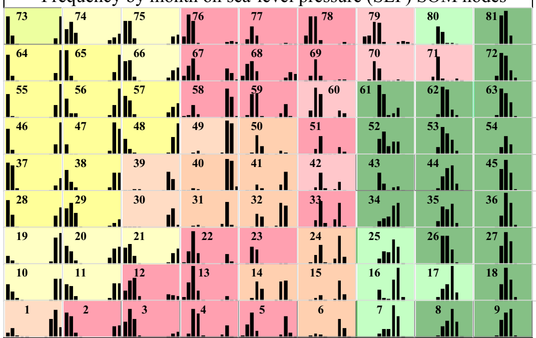

Mean sea-level pressure (mb) on SLP SOM nodes

1019	1017	1016	1014	1011	1010	1009	1006	1003
1019	1018	1017	1014	1012	1010	1008	1007	1005
1018	1017	1016	1014	1012	1009	1007	1006	1004
1018	1017	1016	1014	1010	1009	1008	1005	1004
1016	1017	1015	1014	1011	1009	1007	1006	1005
1016	1015	1015	1013	1011	1009	1007	1007	1005
1015	1015	1015	1013	1011	1010	1008	1006	1006
1015	1014	1013	1012	1012	1011	1009	1008	1007
1013	1014	1014	1013	1015	1012	1010	1008	1007

Mean precipitation (mm/day) on SLP SOM nodes

2.0	1.8	1.8	1.8	1.6	1.7	2.7	4.8	6.3
2.0	1.9	1.9	1.9	1.8	2.3	2.6	3.9	5.8
2.3	2.2	2.0	2.3	2.0	2.7	4.5	5.9	6.0
1.9	2.6	2.2	3.2	2.5	3.6	4.8	5.6	6.1
1.7	1.9	2.4	2.9	3.3	3.7	4.2	5.6	6.1
1.9	1.5	2.7	3.1	3.3	3.8	4.8	5.4	5.9
2.5	1.9	2.0	1.8	1.8	3.5	5.2	5.9	5.9
2.2	2.0	1.6	1.6	3.0	3.5	4.5	5.4	5.6
2.9	1.7	1.4	1.8	1.9	3.3	4.7	5.1	5.3

Color of box denotes seasonal association

Fig. 3 Associated with each of the SOM nodes in Fig. 2: (left) relative monthly frequency by month of each node, from January to December (left to right), (middle) mean sea-level pressure (mb) per node, and (right) mean precipitation (mm) by node. Color of boxes denote seasonal association

northeasterly winds start to be replaced by a pre-monsoon northwesterly wind. When the pre-monsoon circulation patterns yield in April through May during the transition to the monsoon (e.g., nodes 35, 36, 42, 43, 44, and 45), the Arabian Sea branch of wind starts to change its direction from northwesterly to westerly and the Bay of Bengal Branch to southwesterly, and over the Western Ghats and the mid Indian peninsula, the wind blows westerly. Through the course of the monsoon season, subtle changes in the wind can be seen in May through June (e.g., nodes 52, 53, and 54), westerlies and south-westerlies dominate the Arabian Sea and Bay of Bengal branches, respectively, veering to southwesterly over Bangladesh and west Bengal. These winds strengthen in July and August (e.g., nodes 62, 69, and 76), in response to the strong pressure gradient. In the transition to the post-monsoon season (e.g., nodes 51, 59, 66, and 69), the Arabian Sea Branch weakens first, and in dominant post-monsoon nodes in October (e.g., nodes 41, 49, 56, and 57), the Bay of Bengal branch also weakens, and northerly winds predominate over the Arabian Sea branch. The post-monsoon reversal continues into winter with northwesterly to northeasterly winds over much of the domain (e.g., nodes 37, 38, 39, 46, 47, and 48).

4.3 Temperature

The results for the temperature SOM can be found in Figs. 8, 9, and 10, with a seasonal cycle evident in a clockwise fashion around the lattice. Across all nodes throughout the

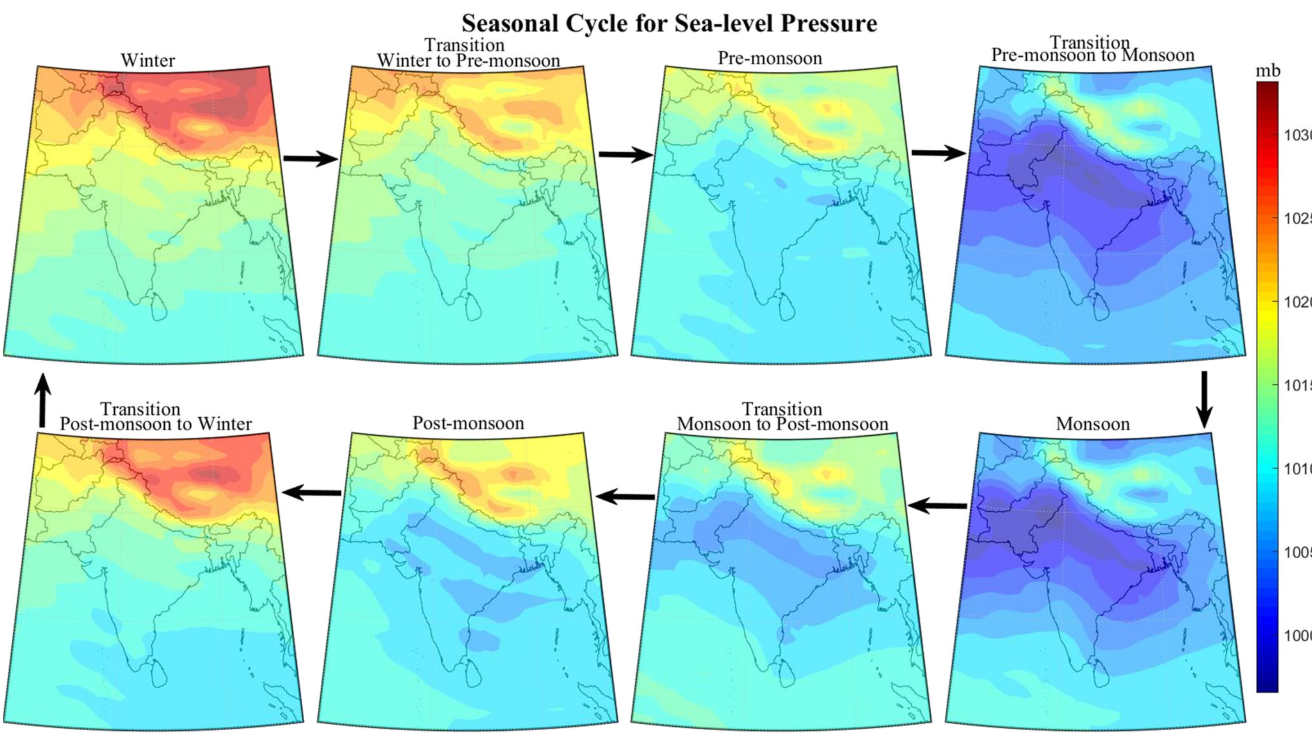

Fig. 4 Each map represents the mean field of SLP across all nodes associated with each season and seasonal transition as depicted in SLP SOM in Fig. 2

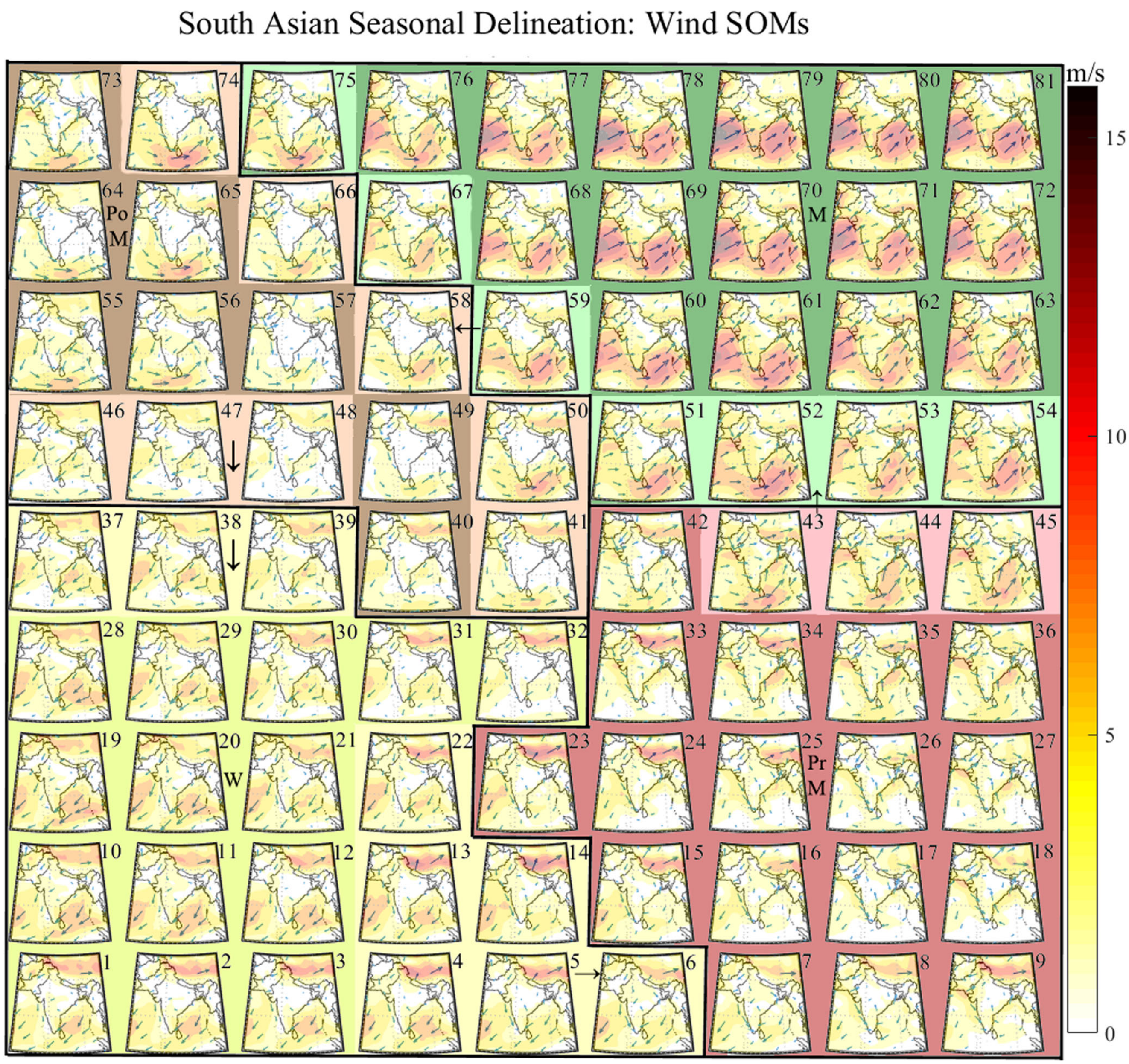

Fig. 5 SOM lattice for wind. Enclosed shade areas denote the different seasons (Pr-M = pre-monsoon (red), M = monsoon (green), Po-M = post-monsoon (brown), and W = winter (yellow), while paler shades of each color denote the transitional nodes and direction of the arrow denotes that the node tend to shift to the following season or fall into the season from prior season

year, the very large spatial gradient of temperature is apparent, with the temperature variability over the Indian Ocean less intense than over the landmass of the Indian peninsula. In the winter (e.g., nodes 31, 32, 33, 34, and 35), aside from the large temperature gradient, the Bay of Bengal Branch is warmer than the shore of the Arabian Sea Branch due to the northwesterly wind that stays over the sea. In the transition to pre-monsoon, the nodes (e.g., 2, 3, 4, 12, and 13) depict a gradual increase of temperature towards the north of the Indian peninsula. The increasing temperature of the land persists through the seasonal transition (e.g., nodes 55, 56, 57, 64, 65, and 73), and by this point, nearly all of the domains have its maximum temperature of the year. In the monsoon season, starting in late June (e.g., nodes 66 and74), the temperature begins to decrease starting with the Western Ghats, and the decreasing trend moves northwestward over the mid-peninsula (e.g., nodes 67, 68, 69, 70, 71, and 72) by July. The transition of monsoon to post-monsoon (e.g., nodes 59, 60, 61, 62, and 63) takes place in September with the decreasing temperature trend continuing southward from the landmass, and by the post-monsoon (e.g., nodes 31, 40, 41, 42, and 43), all areas see markedly decreased temperatures, though there is a slight increase in temperature over the Arabian Sea and Bay of Bengal branches.

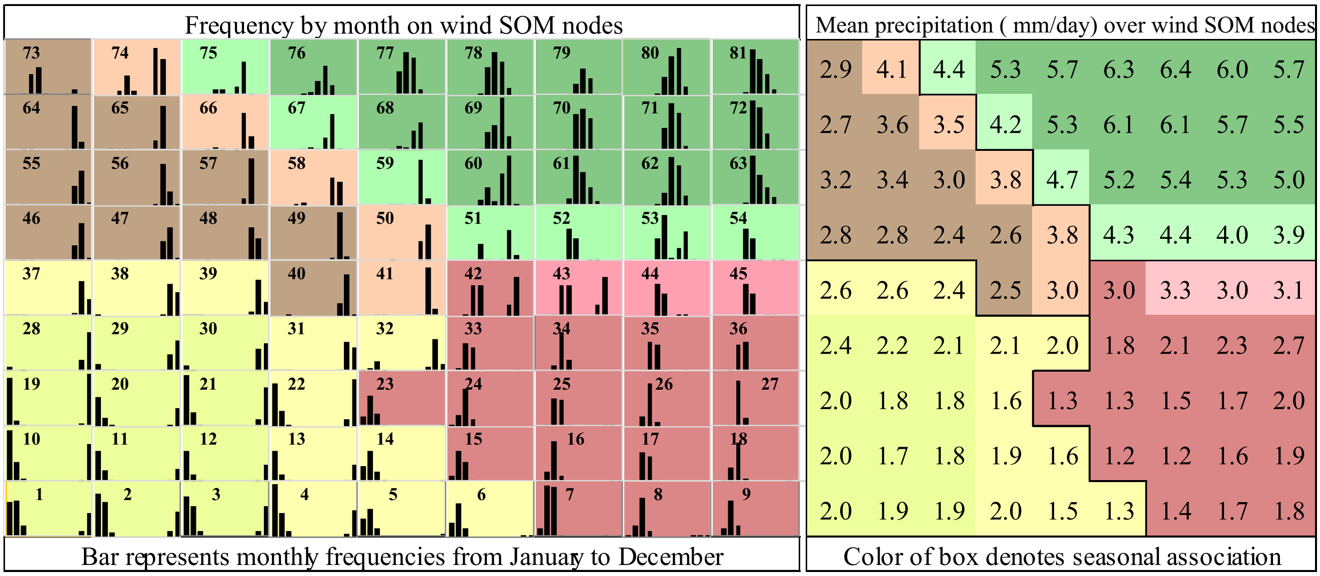

Fig. 6 Associated with each of the SOM nodes in Fig. 5: (left) relative monthly frequency by month of each node, from January to December (left to right) and (right) mean precipitation (mm) by node. Color of boxes denote seasonal association

4.4 Relative humidity

The SOM for relative humidity is shown in Figs. 11, 12, and 13, in which a pronounced seasonal cycle is apparent. The winter nodes (e.g., 28, 37, 46, and 55) depict the starkest contrast, showing dry air over all of the Indian sub-continent, and a sharp gradient along the Indian Ocean coastline. This spatial pattern does not change substantively during the pre-monsoon season (e.g., nodes 1, 2, 12, and 31) with only a slight increase in relative humidity over the land. The transition of pre-monsoon to monsoon in May (e.g., nodes 8, 9, 17, 18, 25, and 26) brings changes, with a large increase over the west coast of the South Indian peninsula as well as the Bay of Bengal, but still low values over the Eastern Ghats along with the coast of the Indian Ocean, as neither the Arabian Sea Branch nor the Bay of Bengal Branch circulation has affected

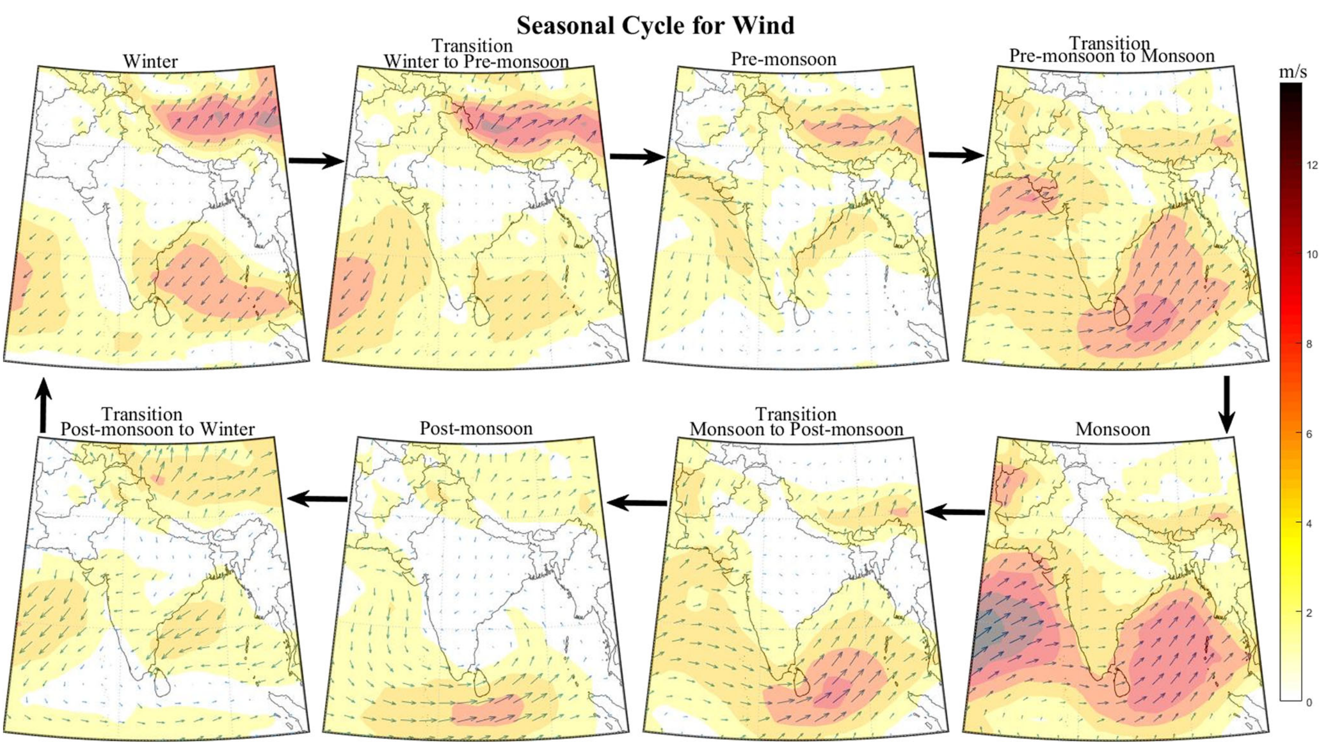

Fig. 7 Each map represents the mean field of wind across all nodes associated with season and seasonal transition as depicted in wind SOM, in Fig. 5

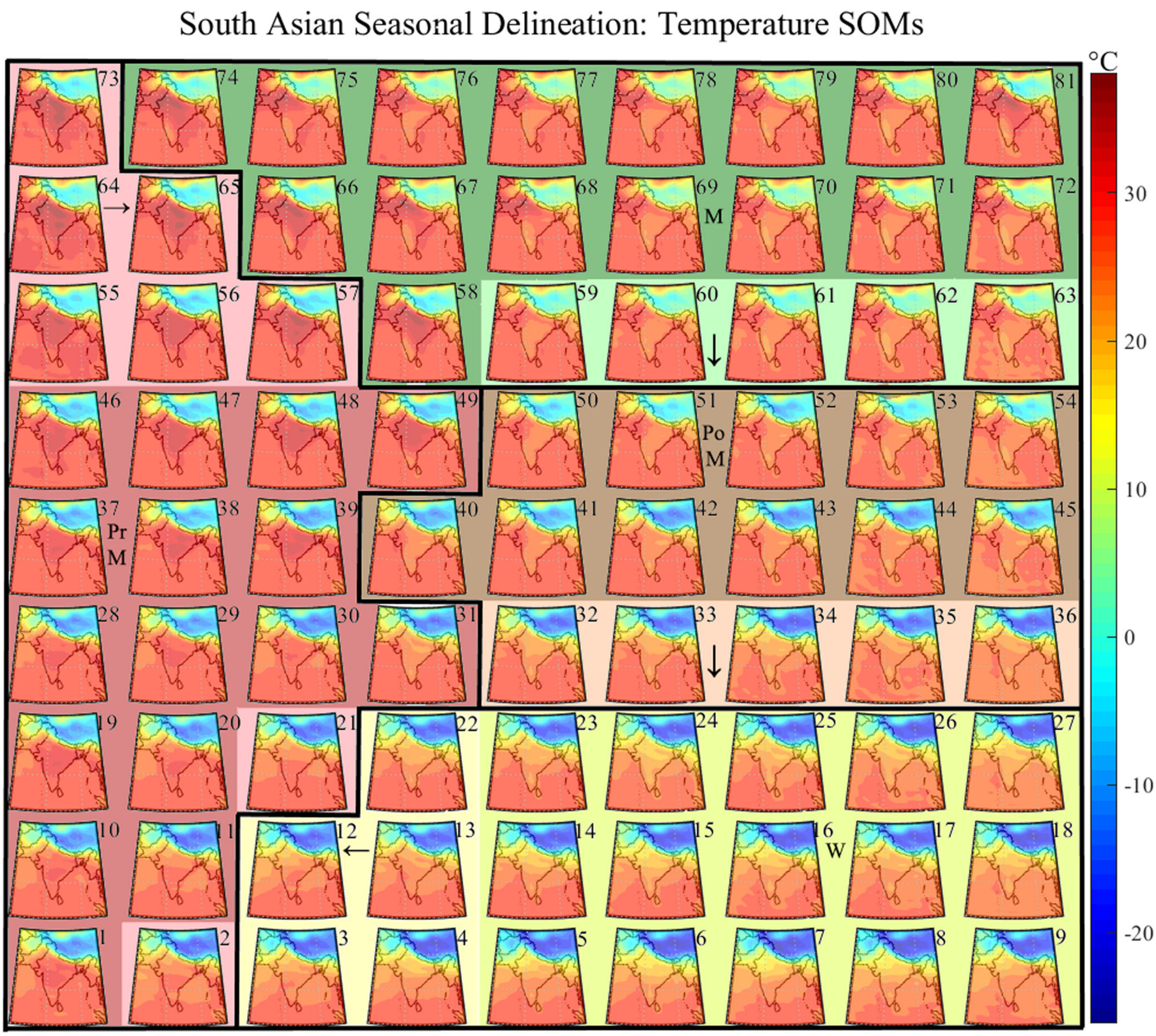

Fig. 8 SOM lattice for temperature. Enclosed shade areas denote the different seasons (Pr-M = pre-monsoon (red), M = monsoon (green), Po-M = post-monsoon (brown), and W = winter (yellow), while paler shades of each color denote the transitional nodes and direction of the arrow denotes that the node tend to shift to the following season or fall into the season from prior season

the area. This changes during the start of the monsoon, in which the circulation shifts to advect moisture over much of the land. In the month of June (e.g., nodes 35, 36, 43, and 44), the monsoonal circulation is fully active over the east and west coast of the Indian peninsula as well as over Bangladesh. In the month of July (e.g., nodes 53 and 54) and August (e.g., nodes 61 and 70), monsoon circulation with high relative humidity has spread all over the central Indian peninsula. These high values over the continent eventually subside in the transition (e.g., nodes 60, 69, and 78) between monsoon and post-monsoon. The gradient of relative humidity from pre-monsoon to monsoon and monsoon to post-monsoon is different due to increased temperature during the transition from pre-monsoon to monsoon compared to that of transition from monsoon to post-monsoon. In the transition of post-monsoon to winter (e.g., nodes 40, 41, 49, 57, 58, 65, 66, and 74), the moisture content drops in the atmosphere, and in the winter (December and January), the relative humidity over the peninsula decreases and stays relatively dry until pre-monsoon.

4.5 Precipitation

Precipitation is one of the most important atmospheric variables used to identify and understand the South Asian summer monsoon. The results of the precipitation SOM (Fig. 14, 15, and 16), show a clear seasonality and a clear spatial distribution of monsoon rainfall over the entire domain. Across the overall array of patterns in the

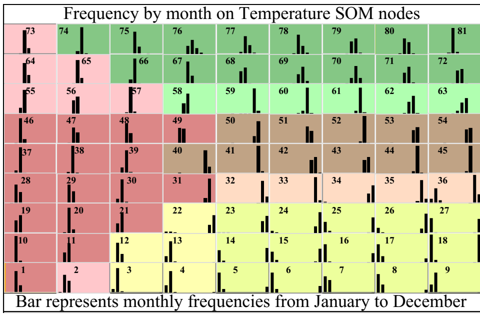

Mean Temperature ° C on Temperature SOM nodes

23.6	24.1	24.1	24.0	23.8	23.7	23.3	23.3	23.3
24.1	23.3	23.7	23.9	23.7	23.3	22.9	23.1	23.1
23.2	22.5	22.7	23.2	22.1	22.0	21.5	22.1	22.2
21.8	21.7	21.7	21.5	20.6	20.8	19.5	20.3	20.2
20.8	21.2	20.3	19.5	19.5	18.1	18.1	17.7	18.3
19.4	19.4	18.0	17.8	17.0	16.4	15.3	16.3	15.6
19.7	18.2	16.9	16.0	15.7	15.4	14.8	14.7	13.7
18.0	16.8	15.7	15.9	14.7	14.6	13.9	14.5	13.6
18.8	16.5	15.0	14.6	13.6	13.6	13.4	12.8	14.2

Mean precipitation (mm/day) over Temperature SOM nodes

16.0	5.0	5.7	5.8	6.0	6.2	5.9	6.1	4.9
3.8	3.6	4.7	5.4	5.9	5.7	5.6	5.9	6.1
2.8	2.4	3.4	4.5	4.3	4.4	4.4	5.1	5.1
2.0	2.4	2.4	3.0	3.5	3.9	3.3	3.8	3.9
1.8	1.9	1.8	3.0	2.9	3.0	2.5	2.7	2.7
1.4	1.8	2.0	2.8	2.8	2.5	2.0	2.1	1.7
1.7	1.3	1.6	2.5	2.4	2.4	2.0	2.0	1.9
1.4	1.4	1.5	1.7	2.2	2.2	1.9	1.6	1.6
1.9	1.4	1.5	1.5	1.9	1.8	1.6	1.4	1.2

Color of box denotes seasonal association

Fig. 9 Associated with each of the SOM nodes in Fig. 8: (left) relative monthly frequency by month of each node, from January to December (left to right), (middle) mean temperature (°C) per node, and (right) mean precipitation (mm) by node. Color of boxes denote seasonal association

SOM, the monsoon season aligns generally along the bottom of the SOM with a smooth seasonal transition. The other three seasons, although less clustered in a specific position in the SOM, can easily be discerned. Within the seasonal cycle, in the transition of post-monsoon to winter (e.g., nodes 54, 62, and 63), the entire landmass receives little precipitation, though the south of Bay of Bengal over the Indian ocean and the east coast of Sri Lanka still receive heavy rainfall, averaging over 15 mm/day with the "northeast monsoon" or "winter monsoon." During the seasonal transition between winter and pre-monsoon (e.g., nodes 64, 65, 73, and 74), the SOM shows a lot of precipitation (10–15 mm/day) over northern Pakistan and Afghanistan which moves towards the eastern Himalayas through February and March, with relatively little precipitation elsewhere, a pattern that extends into the pre-monsoon as well (e.g., nodes 57, 64, 66, and 73). Towards the end of the pre-monsoon, some nodes (e.g., node 51) show heavy precipitation over the seven sister states (e.g., Tripura, Meghalaya, and Assam) of India and rainfall over the northeast part of Bangladesh due to orographic uplift. As the transition progresses (e.g., nodes 35 and 43) between pre-monsoon to monsoon, Kerala starts to get monsoonal rainfall, and from May to June (e.g., nodes 9, 18, 26, and 33), rain-bearing monsoonal rain spreads over the Bay of Bengal and the adjacent region including Myanmar, although topographic barriers limit its extent over the Indian peninsula. By the months of

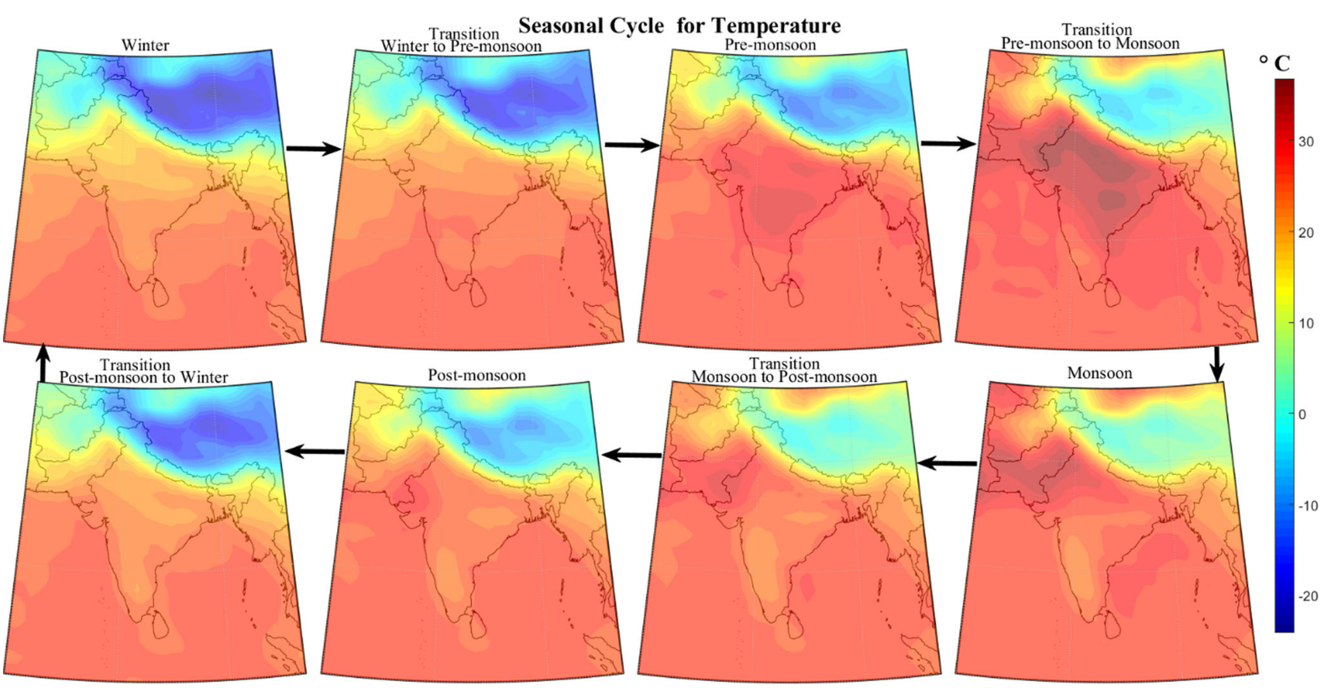

Fig. 10 Each map represents the mean field of temperature across all nodes associated with season and seasonal transition as depicted in temperature SOM in Fig. 8

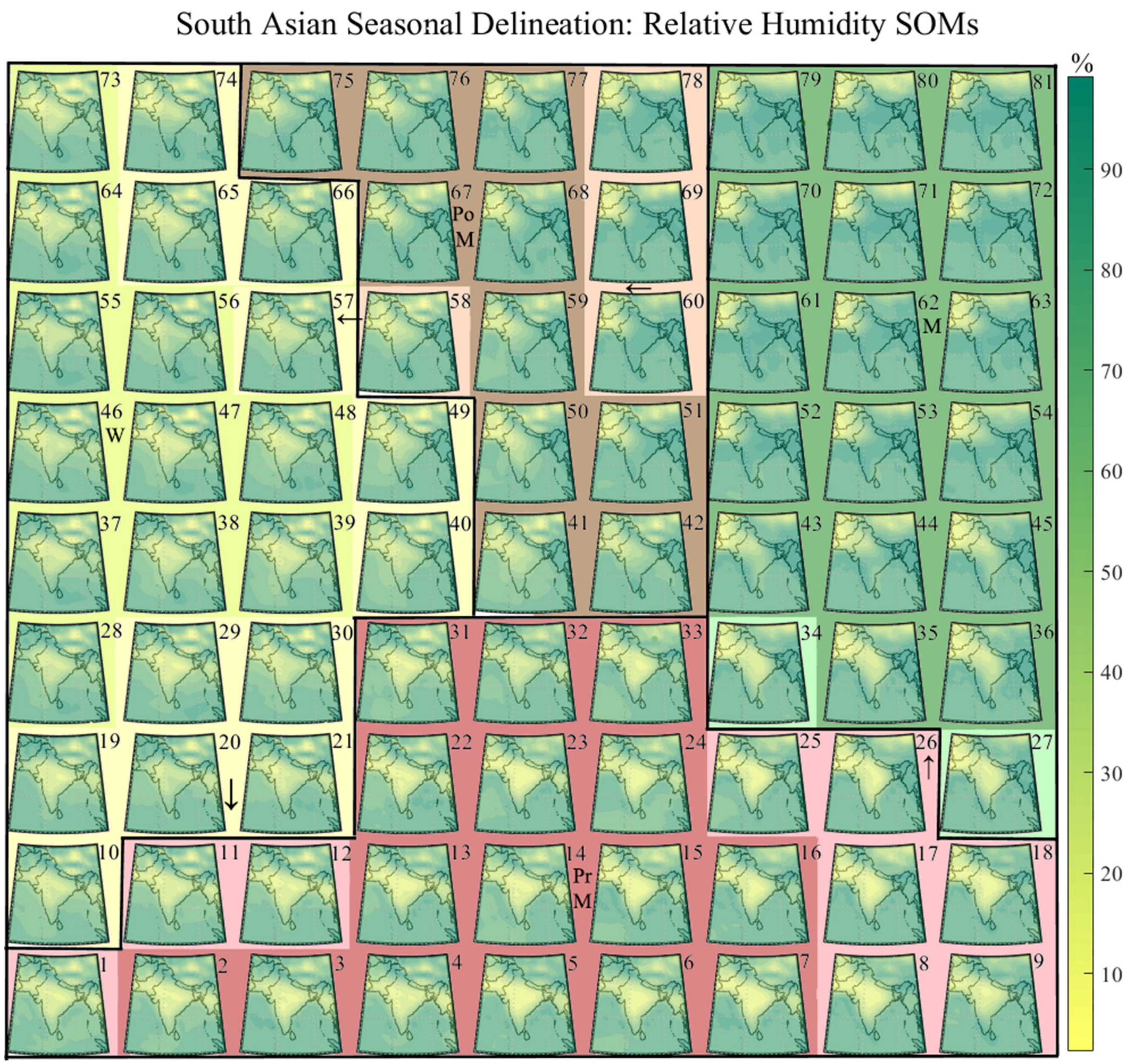

Fig. 11 SOM lattice for relative humidity. Enclosed shade areas denote the different seasons (Pr-M = pre-monsoon (red), M = monsoon (green), Po-M = post-monsoon (brown), and W = winter (yellow), while paler shades of each color denote the transitional nodes and direction of the arrow denotes that the node tend to shift to the following season or fall into the season from prior season

July and August, however (e.g., nodes 1, 2, 3, and 5), substantial rainfall spreads over most parts of the landmass, peaking generally across parts of the Himalayas and the southern coasts, with decreasing amounts in the western deserts. During the transition of monsoon to post-monsoon (e.g., nodes 31, 32, 37, and 38), rainfall starts to decrease over the parts of the Indian landmass, extending further as the season progress to the post-monsoon (e.g., nodes 39, 44, and 48). The cessation of precipitation takes place in the post-monsoon (e.g., node 45) over the entire peninsula while the Eastern Ghats still receives a considerable amount of rainfall.

5 Discussion

5.1 Seasonal delineation

The SOM shows the general climatology of the region through atmospheric patterns, such as a pressure gradient (high to low) gradually extending from north to south until the month of July. In contrast, a complete reversal of the pressure gradient (low to high) starts to take place in the month of August and continue until January. These two stages of complete reversal of sea-level pressure takes place over the Indian sub-continent landmass due to the

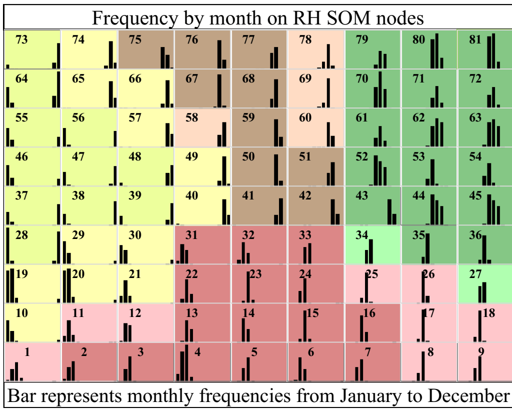

Mean RH (%) on RH SOM nodes

61.8	64.8	67.6	70.2	70.0	70.6	73.0	71.2	73.8
64.5	65.0	68.3	68.6	70.4	71.5	73.6	72.6	75.0
66.9	66.8	65.5	64.7	68.5	72.9	74.7	74.5	73.1
63.4	62.0	65.3	63.8	65.5	69.0	72.8	72.4	71.1
64.9	64.0	62.9	64.3	63.1	66.9	69.2	68.5	69.8
67.2	62.9	63.8	62.6	65.2	61.7	65.0	65.9	68.1
64.8	65.9	65.0	62.1	60.9	60.8	62.6	63.9	66.3
63.2	61.9	61.9	62.6	61.3	61.1	63.7	63.2	64.5
61.0	62.0	64.9	62.6	63.2	63.8	62.0	63.9	66.1

Mean precipitation (mm/day) over RH SOM nodes

2.3	3.0	3.1	3.1	3.8	4.6	5.4	5.8	6.2
2.2	2.3	3.2	3.2	3.6	4.5	5.5	5.6	6.3
2.0	2.3	1.9	2.8	2.8	4.3	5.7	5.4	5.9
1.7	1.9	2.3	2.5	2.6	3.3	5.3	6.1	6.1
2.3	2.1	1.7	1.9	1.6	2.5	5.3	5.5	5.4
2.3	1.7	1.5	1.4	2.0	2.1	4.2	4.7	5.2
1.9	1.8	1.6	1.3	2.0	1.4	2.8	3.5	4.3
1.3	1.3	1.3	1.7	1.4	1.8	2.4	3.3	3.2
1.2	1.3	1.7	1.2	1.7	1.8	1.7	3.1	3.3

Color of box denotes seasonal association for relative humidity (RH)

Fig. 12 Associated with each of the SOM nodes in Fig. 11: (left) relative monthly frequency by month of each node, from January to December (left to right), (middle) mean relative humidity (%) per node, and (right) mean precipitation (mm) by node. Color of boxes denote seasonal association

development of the monsoon trough as a consequence of the northward migration of the inter-tropical convergence zone (ITCZ). The wind SOM shows a climatology with a clear anticyclonic wind movement in winter season and cyclonic wind movement in monsoon season over the both branches, with a greater wind speed prevailing over the sea than the land, triggered by the high-pressure belt over the landmass during the winter and low-pressure belt during the monsoon, respectively. Similar to the climatology of the entire northern hemisphere, the mean South Asian surface temperature rises steadily from late January to late June and decreases from early July to late December. The temperature starts to increase in the transition of winter to pre-monsoon, rises to its peak during the pre-monsoon to monsoon transition in the months of May and June, and stays high into the middle of the monsoon season, before gradually decreasing towards the post-monsoon. The overall array of the relative humidity SOM shows a climatology of the South Asian region well, with humid conditions year around over the Indian Ocean, dry conditions over

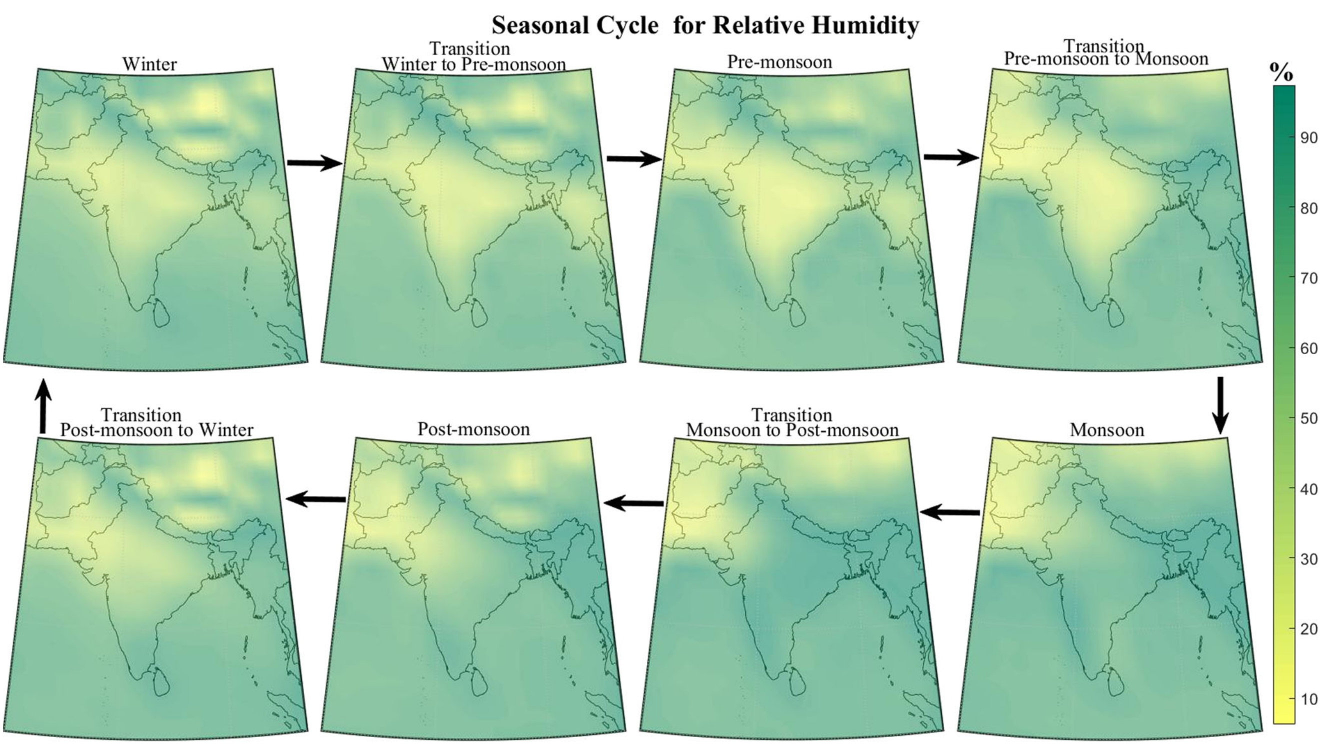

Fig. 13 Each map represents the mean field of relative humidity across all nodes associated with season and seasonal transition as depicted in relative humidity SOM in Fig. 11

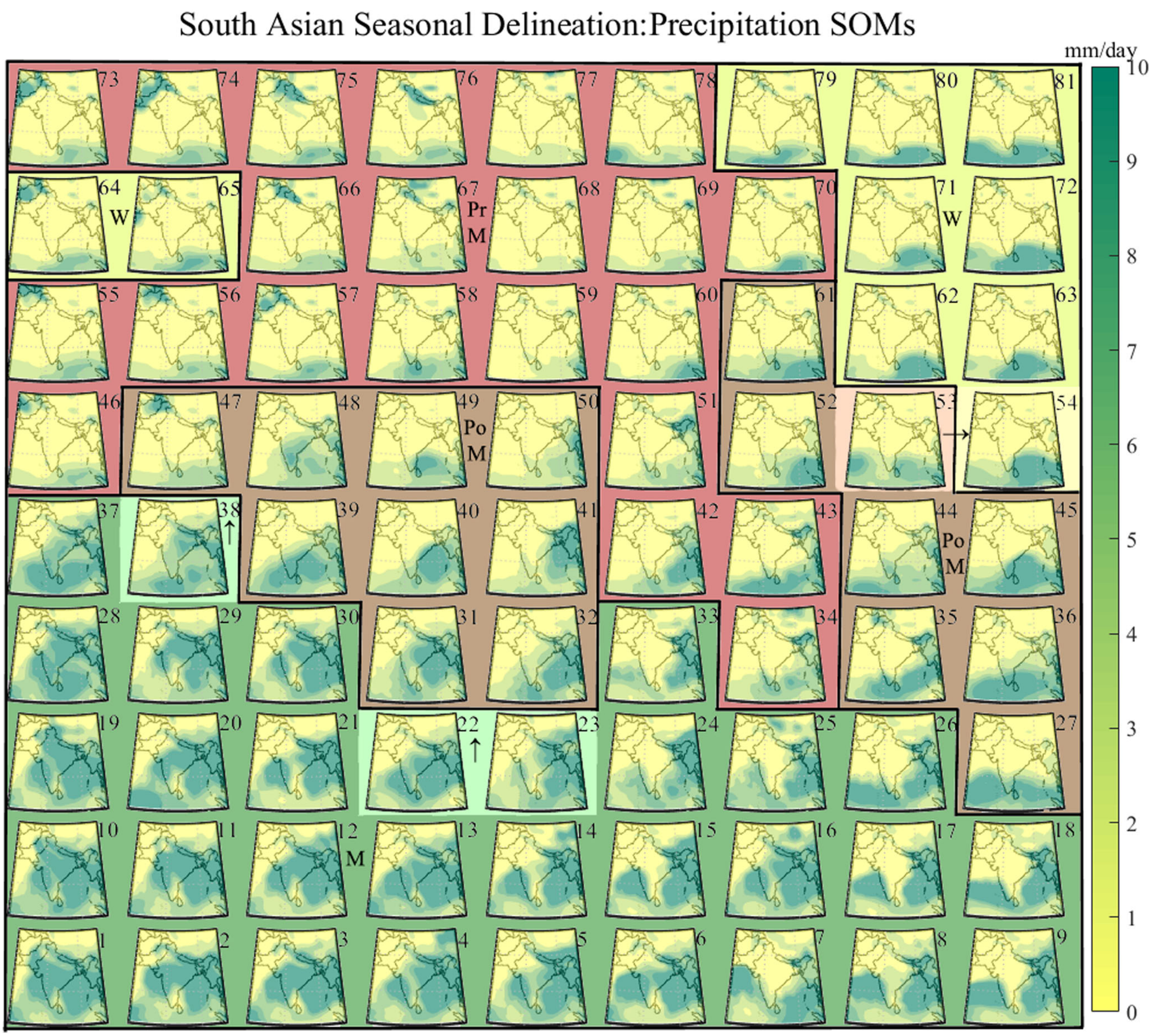

Fig. 14 SOM lattice for precipitation. Enclosed shade areas denote the different seasons (Pr-M = pre-monsoon (red), M = monsoon (green), Po-M = post-monsoon (brown), and W = winter (yellow), while paler shades of each color denote the transitional nodes and direction of the arrow denotes that the node tend to shift to the following season or fall into the season from prior season

Pakistan and northwest India, and a strong seasonality over the rest of the South Asian landmass.

In assessing the seasonality of South Asia, the SOM has a clear ability to partition the seasons by atmospheric patterns for some variables better than others. Overall, the SOMs for wind, relative humidity and temperature have the best visual illustration in terms of seasonality in comparison to the sea-level pressure and precipitation SOMs. Although it has been tested in several ways (e.g., changing dimensions, learning rates, iterations), no permutations were able to separate the pre-monsoon and post-monsoon nodes for sea-level pressure, or the non-monsoon seasons nodes for precipitation. The sea-level pressure SOM ended up with a mixed array due to the similar data values in both pre-monsoon and post-monsoon seasons, and with the precipitation SOM, three seasons (post-monsoon, winter, and pre-monsoon) of failed to organize due to the lack of the variability of precipitation across those seasons, especially compared to the monsoon season. However, the winter and the monsoon patterns of sea-level pressure are organized more logically in that, as one moves from left to right across the SOM array, the nodes depict high pressure in the wintertime over the land and transition gradually to become a low-pressure pattern during monsoon.

The very clear pressure gradient resulting from a distinct high-pressure pattern over the land accompanied by a low-pressure pattern over the ocean in winter, and the opposite occurring during the monsoon season, shows that this

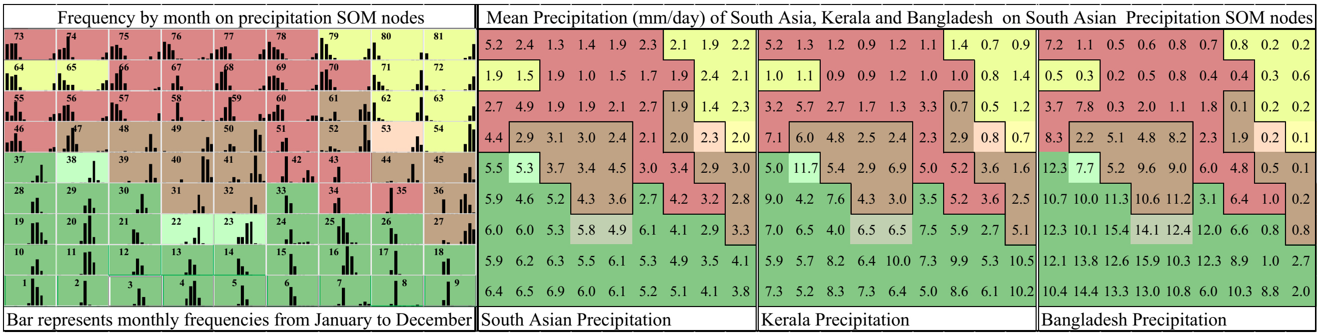

Fig. 15 Associated with each of the SOM nodes in Fig. 14: (left) relative monthly frequency by month of each node, from January to December (left to right), and (right) mean precipitation (mm) by node. Color of boxes denote seasonal association

seasonality of the monsoonal climate system is well defined by the SLP SOM. In contrast, due to the general weakening of both pressure centers, pre-monsoon and post-monsoon seasons are a bit more ill-defined. Similarly, the wind SOM also identifies the winter and monsoon seasons well with strong winds and distinct wind directions across all circulation patterns assigned to the respective season; however, the character of the pre-monsoon and post-monsoon seasons are somewhat more nebulous arising from the weak and variable winds and greater heterogeneity of the circulation patterns assigned to those seasons. In assessing the temperature SOM, the winter and the pre-monsoon seasons show stronger differences than that of the monsoon and the post-monsoon seasons in terms of the average field of temperature. Even though the monsoon season occurs in meteorological summer, the peak temperature occurs in the late pre-monsoon to mid-monsoon season when, based on temperature distribution, the seasonal distinction is more difficult to assess than with other variables, except for winter. In comparison to other variables, a larger number of patterns characterized in the precipitation SOM for monsoon season with distinct seasonal character relative to other seasons, because of the variability of precipitation fields during the monsoon, and the lack of variability in the winter and other seasons. The winter seasonal nodes are separated into two groups in the SOM, adjacent to both the pre-monsoon and post-monsoon seasons. The mean precipitation of the post-monsoon neighboring winter nodes is higher than that of pre-monsoon neighboring winter nodes. Although the other three seasons are generally well separated into cohesive areas of the SOM array, the organization of the seasonal cycle is not as clearly defined as that of wind, temperature, and relative humidity.

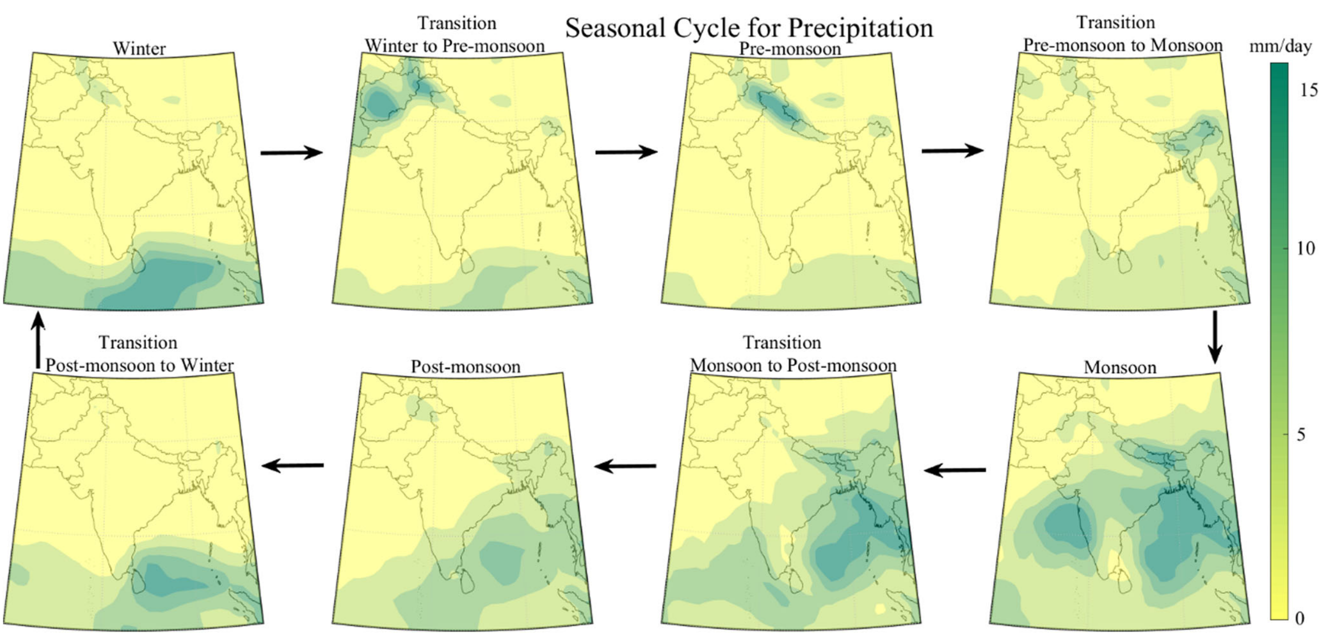

Fig. 16 Each map represents the mean field of precipitation across all nodes associated with season and seasonal transition as depicted in precipitation SOM in Fig. 14

Fig. 17 Mean precipitation by node, based on the sea-level pressure SOM in Fig. 2, for the entire South Asian region, as well as Kerala and Bangladesh

Mean Precipitation (mm) By Sea Level Pressue SOM Node

South Asia

2.0	1.8	1.8	1.8	1.6	1.7	2.7	4.8	6.3
2.0	1.9	1.9	1.9	1.8	2.3	2.6	**3.9**	5.8
2.3	2.2	2.0	2.3	2.0	2.7	4.5	5.9	6.0
1.9	2.6	2.2	3.2	2.5	3.6	4.8	5.6	6.1
1.7	1.9	2.4	2.9	3.3	3.7	4.2	5.6	6.1
1.9	1.5	2.7	3.1	3.3	3.8	4.8	5.4	5.9
2.5	1.9	2.0	1.8	1.8	**3.5**	5.2	5.9	5.9
2.2	2.0	1.6	1.6	3.0	**3.5**	**4.5**	5.4	5.6
2.9	1.7	1.4	1.8	1.9	**3.3**	4.7	5.1	5.3

Kerala

1.1	0.9	0.8	0.8	1.4	1.7	3.9	8.6	8.0
1.3	1.2	1.2	1.7	1.5	3.0	3.6	**4.3**	8.7
2.2	1.4	1.7	3.6	2.6	3.3	7.1	7.5	8.5
1.4	3.0	1.6	5.8	3.4	4.6	6.8	7.7	7.6
0.8	1.1	3.1	4.1	5.0	4.7	5.8	7.2	6.9
1.2	0.9	3.2	4.2	4.3	4.6	6.3	6.7	6.5
2.5	1.8	1.1	1.7	1.7	**4.6**	6.6	6.7	6.0
2.4	1.5	1.3	1.3	4.6	**4.0**	**4.8**	6.0	5.8
4.4	1.1	0.7	1.9	1.8	**4.1**	4.9	5.5	5.1

Bangladesh

0.2	0.5	0.1	0.4	0.8	1.2	2.5	8.1	12.4
0.3	0.2	0.3	1.1	0.7	3.3	3.7	**5.6**	11.4
0.3	0.2	0.4	2.1	2.1	3.9	8.3	13.7	10.7
0.1	0.4	0.2	3.2	4.1	5.5	10.2	10.3	12.7
0.1	0.5	2.3	1.8	4.8	7.3	6.8	10.8	12.8
0.3	0.3	1.4	4.5	5.7	6.3	9.7	10.2	14.4
0.3	0.3	0.2	0.9	1.8	**7.8**	11.5	14.0	13.9
0.3	0.2	1.0	0.7	6.5	**7.7**	**9.5**	11.5	14.2
0.8	0.2	0.2	1.6	1.6	**7.5**	10.7	13.4	12.5

Node 71 disputed nodes (bold) considered as pre-monsoon node, mean precipitation is less than any of monsoon nodes

5.2 Synoptic validation

In this research, the self-organizing maps technique identified an interesting relationship between South Asian sub-continental scale atmospheric patterns and local to regional-scale precipitation environments. Two important regional places taken into consideration are (1) Kerala, the gateway to the monsoon season and representative of the Arabian Sea Branch of the monsoon in South Asia, and (2) Bangladesh, the delta funnel as well the key location for the Bay of Bengal branch of monsoon seasonal circulation. SOMs demonstrate a consistent relationship between the South Asian sub-continental scale atmospheric pattern and the local- to regional-scale (Kerala and Bangladesh) environment, both in terms of the mean field of atmospheric conditions and average precipitation of corresponding nodes of the precipitation-based SOM (Fig. 16). Thus, the sub-continental scale atmospheric patterns successfully represent broadly homogenous characteristics, which can affect the local-scale atmospheric patterns. For instance, Kerala and Bangladesh average precipitation fields over each of the corresponding SOMs nodes of different atmospheric variables show that the South Asian sub-continental scale atmospheric patterns are key drivers of local-scale precipitation variability and are able to clearly delineate seasonal differences in precipitation (Fig. 17). The synoptic responses (node to node) are similar to the large-scale sub-continental and local scale of circulations in relation to the threshold mean field of a particular variable in terms of seasons. These similarities illustrate the consistent relationship between the larger scale circulations and the regional climate, increase our understanding of the evolution of the monsoon system, and highlight the utility of the synoptic methodology in analyzing the monsoon system.

6 Conclusion

The key findings of this research are the following:

- This research has demonstrated a new application of the synoptic approach (specifically atmospheric patterns) as a way to understand the seasonality of the South Asian climate.
- Self-organizing maps (SOMs) help to illustrate the general climatology of the region by displaying the smooth flow of various atmospheric variables through four well-defined seasons including their transitions. This research not only delineates seasons, but also demonstrates the seasonal cycle of the regional climate system.
- The SOM classifies the synoptic atmospheric patterns in such a way that the general characteristics of atmospheric conditions for a particular season not only reflect the sub-continental climate as a whole but also can impact local climate in terms of mean fields of precipitation.

Future research will use these seasonal classifications to determine the onset and withdrawal dates in South Asian seasons. Analyzing the frequencies of nodes and lengths of the seasons, we can also understand the impact of climate change in this region.

References

Alexander LV, Uotila P, Nicholls N, Lynch A (2010) A new daily pressure dataset for Australia and its application to the assessment of changes in synoptic patterns during the last century. J Clim 23(5):1111–1126

Barry RG, Perry AH (1973a) Synoptic climatology; methods and applications. Routledge and Kegan Paul, London

Barry RG, Perry AH (1973b) Synoptic climatology: methods and applications. Methuen, London

Barry R, Perry A (2001) Synoptic climatology and its applications. Synoptic and Dynamic Climatology. Routledge, New York, pp 547–603

Bhalme HN, Rahalkar SS, and Sikder AB (1987) Tropical Quasi-Biennial Oscillation of the 10-mb wind and Indian monsoon rainfall-implications for forecasting. Journal of climatology 7(4):345–353

Cassano EN, Cassano JJ (2010) Synoptic forcing of precipitation in the Mackenzie and Yukon river basins. Int J Climatol 30(5):658–674

Cassano EN, Lynch AH, Cassano JJ, Koslow MR (2005) Classification of synoptic patterns in the Western Arctic associated with extreme events at barrow, Alaska, USA. Clim Res 30(2):83

Cassano JJ, Uotila P, Lynch A (2006) Changes in synoptic weather patterns in the polar regions in the twentieth and twenty-first centuries, part 1: Arctic. Int J Climatol 26(8):1027–1049

Cassano EN, Glisan JM, Cassano JJ, Gutowski WJ Jr, Seefeldt MW (2015) Self-organizing map analysis of widespread temperature extremes in Alaska and Canada. Clim Res 62(3):199–218

Cassano EN et al (2017) Synoptic conditions during summertime temperature extremes in Alaska. Int J Climatol 37(9):3694–3713

Cavazos T (2000) Using self-organizing maps to investigate extreme climate events: an application to wintertime precipitation in the Balkans. J Clim 13(10):1718–1732

Cavazos T, Comrie AC, Liverman DM (2002) Intraseasonal variability associated with wet monsoons in Southeast Arizona. J Clim 15(17): 2477–2490

Chattopadhyay R, Sahai A, Goswami BN (2008) Objective identification of nonlinear convectively coupled phases of monsoon intraseasonal oscillation: implications for prediction. J Atmos Sci 65(5):1549–1569

Crane RG, Hewitson BC (2003) Clustering and upscaling of station precipitation records to regional patterns using self-organizing maps (SOMs). Clim Res 25(2):95–107

Deme A, Viltard A, de Félice P (2003) Daily precipitation forecasting in Dakar using the NCEP-NCAR reanalyses. Weather Forecast 18(1): 93–105

Demuzere M et al (2009) An analysis of present and future ECHAM5 pressure fields using a classification of circulation patterns. Int J Climatol 29(12):1796–1810

Finnis J, Cassano J, Holland M, Serreze M, Uotila P (2009) Synoptically forced hydroclimatology of major arctic watersheds in general circulation models; part 1: the Mackenzie River basin. Int J Climatol 29(9):1226–1243

Gibson PB, Perkins-Kirkpatrick SE, Uotila P, Pepler AS, Alexander LV (2017) On the use of self-organizing maps for studying climate extremes. J Geophys Res Atmos 122:3891–3903

Gueye A et al (2011) Weather regimes over Senegal during the summer monsoon season using self-organizing maps and hierarchical ascendant classification. Part I: synoptic time scale. Clim Dyn 36(1–2):1–18

Hewitson B, Crane R (2002) Self-organizing maps: applications to synoptic climatology. Clim Res 22(1):13–26

Hope PK, Drosdowsky W, Nicholls N (2006) Shifts in the synoptic systems influencing Southwest Western Australia. Clim Dyn 26(7–8): 751–764

Horton DE, Johnson NC, Singh D, Swain DL, Rajaratnam B, Diffenbaugh NS (2015) Contribution of changes in atmospheric circulation patterns to extreme temperature trends. Nature 522(7557):465–469. https://doi.org/10.1038/nature14550

Janowiak JE, Gruber A, Kondragunta CR, Livezey RE, Huffman GJ (1998) A comparison of the NCEP–NCAR reanalysis precipitation and the GPCP rain gauge–satellite combined dataset with observational error considerations. J Clim 11(11):2960–2979

Kalnay E et al (1996) The NCEP/NCAR 40-year reanalysis project. Bull Am Meteorol Soc 77(3):437–471

Kohonen T (1998) The self-organizing map. Neurocomputing 21(1):1–6

Kripalani RH, Kulkarni A, Sabade SS (2003) Western Himalayan snow cover and Indian monsoon rainfall: a re-examination with INSAT and NCEP/NCAR data. Theor Appl Climatol 74(1):1–18

Krishnamurthy V, Shukla J (2000) Intraseasonal and interannual variability of rainfall over India. J Clim 13(24):4366–4377

Kumar KK, Soman MK, Kumar KR (1995) Seasonal forecasting of Indian summer monsoon rainfall: a review. Weather 50(12):449–467

Lee CC, Sheridan SC (2015): Synoptic Climatology: An Overview. Reference Module in Earth Systems and Environmental Sciences. Elsevier https://doi.org/10.1016/B978-0-12-409548-9.09421-5

Lynch A, Uotila P, Cassano JJ (2006) Changes in synoptic weather patterns in the polar regions in the twentieth and twenty-first centuries, part 2: Antarctic. Int J Climatol 26(9):1181–1199

Michaelides SC, Pattichis CS, Kleovoulou G (2001) Classification of rainfall variability by using artificial neural networks. Int J Climatol 21(11):1401–1414

Mukherjee BK et al (1985) Quasi-biennial oscillation in stratospheric zonal wind and Indian summer monsoon. Mon Weather Rev 113(8): 1421–1424

Pant GB, Kumar KR (1997) Climates of South Asia. Wiley, Chichester

Ramage CS (1971) Monsoon meteorology. No. 551.518 R3

Rao KG, Goswami BN (1988) Interannual variations of sea surface temperature over the Arabian Sea and the Indian monsoon: a new perspective. Mon Weather Rev 116(3):558–568

Rasmusson EM, Carpenter TH (1982) Variations in tropical sea surface temperature and surface wind fields associated with the Southern Oscillation/El Niño. Mon Weather Rev 110(5):354–384

Schuenemann KC, Cassano JJ (2009) Changes in synoptic weather patterns and Greenland precipitation in the 20th and 21st centuries. 10th conference on polar meteorology and oceanography

Sheridan SC (2002) The redevelopment of a weather-type classification scheme for North America. International Journal of Climatology: A Journal of the Royal Meteorological Society 22(1):51–68

Sheridan SC, Lee CC (2010) Synoptic climatology and the general circulation model. Prog Phys Geogr 34(1):101–109

Sheridan SC, Lee CC (2011) The self-organizing map in synoptic climatological research. Prog Phys Geogr 35(1):109–119

Sheridan SC, Lee CC (2014) "Synoptic climatology." Oxford bibliographies in geography. Oxford University Press, New York. https://doi.org/10.1093/OBO/9780199874002-0088

Swales D, Alexander M, Hughes M (2016) Examining moisture pathways and extreme precipitation in the U.S. intermountain west using self-organizing maps. Geophys Res Lett 43:1727–1735. https://doi.org/10.1002/2015GL067478

Tozuka T, Luo J, Masson S, Yamagata T (2008) Tropical Indian ocean variability revealed by self-organizing maps. Clim Dyn 31(2–3): 333–343

Verdon-Kidd D, Kiem A (2009) On the relationship between large-scale climate modes and regional synoptic patterns that drive Victorian rainfall. Hydrol Earth Syst Sci 13(4):467–479

Yarnal B (1993) Synoptic climatology in environmental analysis: A primer. Belhaven press, London